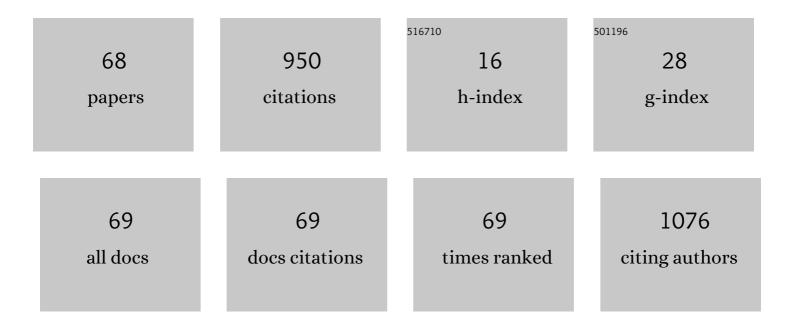
Terumitsu Hasebe

List of Publications by Year in descending order

Source: https://exaly.com/author-pdf/2573570/publications.pdf Version: 2024-02-01



TEDIIMITSII HASERE

#	Article	IF	CITATIONS
1	Diamond-like carbon films for PET bottles and medical applications. Thin Solid Films, 2006, 494, 84-91.	1.8	182
2	Fluorine doping into diamond-like carbon coatings inhibits protein adsorption and platelet activation. Journal of Biomedical Materials Research - Part A, 2007, 83A, 1192-1199.	4.0	83
3	Fracture mechanics of diamond-like carbon (DLC) films coated on flexible polymer substrates. Surface and Coatings Technology, 2007, 201, 6423-6430.	4.8	58
4	Oxygen transmission of transparent diamond-like carbon films. Diamond and Related Materials, 2005, 14, 1112-1115.	3.9	39
5	Depth profiling of fluorine-doped diamond-like carbon (F-DLC) film: Localized fluorine in the top-most thin layer can enhance the non-thrombogenic properties of F-DLC. Thin Solid Films, 2007, 516, 299-303.	1.8	34
6	Accuracy of realâ€time magnetic resonance imagingâ€transrectal ultrasound fusion imageâ€guided transperineal target biopsy with needle tracking with a mechanical positionâ€encoded stepper in detecting significant prostate cancer in biopsyâ€naÃ⁻ve men. International Journal of Urology, 2017, 24, 288-294.	1.0	32
7	Balloon-occluded transarterial chemoembolization using a 1.8-French tip Coaxial microballoon catheter for hepatocellular carcinoma: Technical and safety considerations. Minimally Invasive Therapy and Allied Technologies, 2015, 24, 94-100.	1.2	28
8	Focal therapy with high-intensity focused ultrasound for the localized prostate cancer for Asian based on the localization with MRI-TRUS fusion image-guided transperineal biopsy and 12-cores transperineal systematic biopsy: prospective analysis of oncological and functional outcomes. International Journal of Clinical Oncology, 2020, 25, 1844-1853.	2.2	28
9	Identification of citrullinated eukaryotic translation initiation factor 4G1 as novel autoantigen in rheumatoid arthritis. Biochemical and Biophysical Research Communications, 2006, 341, 94-100.	2.1	27
10	Hydrophobicity and non-thrombogenicity of nanoscale dual rough surface coated with fluorine-incorporated diamond-like carbon films: Biomimetic surface for blood-contacting medical devices. Diamond and Related Materials, 2013, 38, 14-18.	3.9	25
11	Gas barrier properties and periodically fractured surface of thin DLC films coated on flexible polymer substrates. Surface and Coatings Technology, 2007, 201, 6431-6436.	4.8	23
12	Simple Fabrication of Gd(III)-DTPA-Nanodiamond Particles by Chemical Modification for Use as Magnetic Resonance Imaging (MRI) Contrast Agent. Applied Physics Express, 2013, 6, 015001.	2.4	23
13	Reduction of severe acute respiratory syndrome coronavirusâ€2 infectivity by admissible concentration of ozone gas and water. Microbiology and Immunology, 2021, 65, 10-16.	1.4	23
14	Ultrastructural characterization of surfaceâ€induced platelet activation on artificial materials by transmission electron microscopy. Microscopy Research and Technique, 2013, 76, 342-349.	2.2	22
15	Controlled formation of wrinkled diamond-like carbon (DLC) film on grooved poly(dimethylsiloxane) substrate. Diamond and Related Materials, 2012, 22, 48-51.	3.9	21
16	Preparation and characterization of 2â€methacryloyloxyethyl phosphorylcholine polymer nanofibers prepared via electrospinning for biomedical materials. Journal of Applied Polymer Science, 2014, 131, .	2.6	21
17	Balloon-occluded arterial stump pressure before balloon-occluded transarterial chemoembolization. Minimally Invasive Therapy and Allied Technologies, 2016, 25, 22-28.	1.2	15
18	Micropatterning of a 2-methacryloyloxyethyl phosphorylcholine polymer surface by hydrogenated amorphous carbon thin films for endothelialization and antithrombogenicity. Acta Biomaterialia, 2019, 87, 187-196.	8.3	15

TERUMITSU HASEBE

#	Article	IF	CITATIONS
19	Basic Fibroblast Growth Factor as a Potential Stent Coating Material Inducing Endothelial Cell Proliferation. Journal of Atherosclerosis and Thrombosis, 2014, 21, 477-485.	2.0	12
20	<i>In vitro</i> basic fibroblast growth factor (bFGF) delivery using an antithrombogenic 2â€methacryloyloxyethyl phosphorylcholine (MPC) polymer coated with a micropatterned diamondâ€like carbon (DLC) film. Journal of Biomedical Materials Research - Part A, 2017, 105, 3384-3391.	4.0	12
21	Comparative performance analysis of interventional devices for the treatment of ischemic disease in below-the-knee lesions: a systematic review and meta-analysis. Cardiovascular Intervention and Therapeutics, 2022, 37, 145-157.	2.3	11
22	Transnodal lymphangiography and post-CT for protein-losing enteropathy in Noonan syndrome. Minimally Invasive Therapy and Allied Technologies, 2015, 24, 246-249.	1.2	10
23	Prospective multi-center registry to evaluate efficacy and safety of the newly developed diamond-like carbon-coated cobalt–chromium coronary stent system. Cardiovascular Intervention and Therapeutics, 2017, 32, 225-232.	2.3	10
24	Hepatic Arterial Infusion Chemotherapy by the Fixed-Catheter-Tip Method: Retrospective Comparison of Percutaneous Left Subclavian and Femoral Port-Catheter System Implantation. American Journal of Roentgenology, 2014, 202, 211-215.	2.2	9
25	Feasibility and Safety of CT-guided Intrathoracic and Bone Re-biopsy for Non-small Cell Lung Cancer. Anticancer Research, 2018, 38, 3587-3592.	1.1	9
26	Prediction of binding characteristics between von Willebrand factor and platelet glycoprotein IbÎ \pm with various mutations by molecular dynamic simulation. Thrombosis Research, 2019, 184, 129-135.	1.7	9
27	Effectiveness of combined use of imprint cytological and histological examination in CT-guided tissue-core biopsy. European Radiology, 2014, 24, 1127-1134.	4.5	8
28	Potential different impact of inhibition of thrombin function and thrombin generation rate for the growth of thrombi formed at site of endothelial injury under blood flow condition. Thrombosis Research, 2019, 179, 121-127.	1.7	8
29	Fabrication of radiopaque drug-eluting beads based on Lipiodol/biodegradable-polymer for image-guided transarterial chemoembolization of unresectable hepatocellular carcinoma. Polymer Degradation and Stability, 2020, 175, 109106.	5.8	8
30	Fabrication of Gd-DOTA-functionalized carboxylated nanodiamonds for selective MR imaging (MRI) of the lymphatic system. Nanotechnology, 2021, 32, 235102.	2.6	8
31	Poly(2-methacryloyloxyethyl phosphorylcholine) (MPC) nanofibers coated with micro-patterned diamond-like carbon (DLC) for the controlled drug release. Journal of Biorheology, 2015, 29, 51-55.	0.5	7
32	A Stepwise Embolization Strategy for a Bronchial Arterial Aneurysm: Proximal Coil and Distal Glue with the Optional Use of a Microballoon Occlusion System. CardioVascular and Interventional Radiology, 2018, 41, 1267-1273.	2.0	7
33	Analysis of oncological outcomes of whole-gland therapy with high-intensity focused ultrasound for localized prostate cancer in clinical and technical aspects: a retrospective consecutive case-series analysis with a median 5-year follow-up. International Journal of Hyperthermia, 2021, 38, 1205-1216.	2.5	7
34	CT-guided bone biopsy using electron density maps from dual-energy CT. Radiology Case Reports, 2021, 16, 2343-2346.	0.6	7
35	Gadolinium-Complexed Carboxylated Nanodiamond Particles for Magnetic Resonance Imaging of the Lymphatic System. ACS Applied Nano Materials, 2021, 4, 1702-1711.	5.0	7
36	Right Aortic Arch with Mirror-image Branching in Adults: Evaluation Using CT. Tokai Journal of Experimental and Clinical Medicine, 2018, 43, 30-37.	0.4	7

TERUMITSU HASEBE

#	Article	IF	CITATIONS
37	Perirenal lymphatic systems: Evaluation using spectral presaturation with inversion recovery <i>T</i> ₂ â€weighted MR images with 3D volume isotropic turbo spinâ€echo acquisition at 3.0T. Journal of Magnetic Resonance Imaging, 2016, 44, 897-905.	3.4	6
38	CT Fluoroscopy-Guided Transsacral Intervertebral Drainage for Pyogenic Spondylodiscitis at the Lumbosacral Junction. CardioVascular and Interventional Radiology, 2017, 40, 125-129.	2.0	6
39	Microballoon-related interventions in various endovascular treatments of body trunk lesions. Minimally Invasive Therapy and Allied Technologies, 2018, 27, 2-10.	1.2	6
40	Pulmonary perfusion by chest digital dynamic radiography: Comparison between breathâ€holding and deepâ€breathing acquisition. Journal of Applied Clinical Medical Physics, 2020, 21, 247-255.	1.9	6
41	The property of adhesion and biocompatibility of silicon and fluorine doped diamond-like carbon films. Diamond and Related Materials, 2021, 119, 108558.	3.9	6
42	Development of a Portable Training Tool for Simulating Visceral Angiographic Procedures for Beginners. CardioVascular and Interventional Radiology, 2009, 32, 412-416.	2.0	5
43	First experience of efficacy and radiation exposure in 320-detector row CT fluoroscopy-guided interventions. British Journal of Radiology, 2021, 94, 20200754.	2.2	5
44	Transcatheter arterial embolization for unruptured renal angiomyolipoma using a 1.8-Fr tip microballoon catheter with a mixture of ethanol and Lipiodol. CVIR Endovascular, 2020, 3, 3.	1.1	5
45	Balloon-occluded retrograde transvenous obliteration using a new microballoon for gastric varices. Minimally Invasive Therapy and Allied Technologies, 2017, 26, 177-181.	1.2	4
46	Can the Number of Radiofrequency Activations Predict Serious Adverse Events after Bronchial Thermoplasty? A Retrospective Case-Control Study. Pulmonary Therapy, 2019, 5, 221-233.	2.2	4
47	Lymphangiography and Post-lymphangiographic Multidetector CT for Preclinical Lymphatic Interventions in a Rabbit Model. CardioVascular and Interventional Radiology, 2019, 42, 448-454.	2.0	4
48	A method and preliminary results of <i>in silico</i> computer simulation for the formation of mix thrombi with platelet and fibrin. Journal of Biorheology, 2017, 31, 30-34.	0.5	4
49	Feasibility and Safety of Repeated Transarterial Chemoembolization Using Miriplatin–Lipiodol Suspension for Hepatocellular Carcinoma. Anticancer Research, 2017, 37, 3183-3187.	1.1	4
50	Do we need a special issue about cutting edges?. Minimally Invasive Therapy and Allied Technologies, 2018, 27, 1-1.	1.2	3
51	Vessel Occlusion using Hydrogel-Coated versus Nonhydrogel Embolization Coils in Peripheral Arterial Applications: A Prospective, Multicenter, Randomized Trial. Journal of Vascular and Interventional Radiology, 2021, 32, 602-609.e1.	0.5	3
52	Detection of Shunting Into Pulmonary Artery on Multidetector Row Computed Tomography Arteriography Before Bronchial Arterial Embolization: A Preliminary Study. Journal of Computer Assisted Tomography, 2020, 44, 852-856.	0.9	3
53	Diamond-Like Carbon and Fluorinated Diamond-Like Carbon Films for Cardiovascular Medical Devices. Hyomen Gijutsu/Journal of the Surface Finishing Society of Japan, 2005, 56, 897-897.	0.2	2
54	The Role of Divided Injections of a Sclerotic Agent over Two Days in Balloon-Occluded Retrograde Transvenous Obliteration for Large Gastric Varices. Korean Journal of Radiology, 2013, 14, 439.	3.4	2

TERUMITSU HASEBE

#	Article	IF	CITATIONS
55	Swine model of in-stent stenosis in the iliac artery evaluating the serial time course. Experimental Animals, 2018, 67, 501-508.	1.1	2
56	The approach of scratchâ€imprint cytology: Is it an alternative to frozen section for intraoperative assessment of pulmonary lesions?. Pathology International, 2020, 70, 31-39.	1.3	2
57	Snuff box radial access in transcatheter arterial embolization for unruptured renal angiomyolipoma. Minimally Invasive Therapy and Allied Technologies, 2021, 30, 27-32.	1.2	2
58	Neoadjuvant chemoradiotherapy for locally advanced gastric cancer with bulky lymph node metastasis: Five case reports. World Journal of Clinical Cases, 2020, 8, 4177-4185.	0.8	2
59	In Vitro Model for Simulating Drug Delivery during Balloon-Occluded Transarterial Chemoembolization. Biology, 2021, 10, 1341.	2.8	2
60	Sporadic gastric neurofibroma underneath early cancer: MDCT gastrography and histological findings. Radiation Medicine, 2007, 25, 236-239.	0.8	1
61	Towards the Next Generation of Implantable Biomedical Devices Using Diamond-Like Carbon Coatings. Hyomen Cijutsu/Journal of the Surface Finishing Society of Japan, 2008, 59, 363-363.	0.2	1
62	Combination therapy using PSE and TIO ameliorates hepatic encephalopathy due to intrahepatic portosystemic venous shunt in idiopathic portal hypertension. Acta Radiologica Open, 2016, 5, 205846011666657.	0.6	1
63	Radiopaque and biodegradable beads fabricated with Lipiodol and polycaprolactone for transarterial chemoembolization. MRS Advances, 2019, 4, 1187-1192.	0.9	1
64	CT fluoroscopy-guided percutaneous intervertebral drain insertion for cervical pyogenic spondylodiscitis. Diagnostic and Interventional Radiology, 2021, 27, 269-271.	1.5	1
65	Pelvic local recurrence as first relapse predicts prognosis for clinical stageÂll/III lower rectal cancer: A clinicopathological investigation. Molecular and Clinical Oncology, 2020, 14, 33.	1.0	1
66	Anti-bacterial property of Hydrogen-free amorphous carbon coatings on Ar plasma-pretreated polytetrafluoroethylene (PTFE) with a-C:H:F interlayer. Materials Research Society Symposia Proceedings, 2013, 1505, 1.	0.1	0
67	Internal biliary drainage for isolated posterior segmental biliary obstruction: a case report. Journal of Medical Case Reports, 2018, 12, 156.	0.8	0
68	Dose length product and outcome of CT fluoroscopy-guided interventions using a new 320-detector row CT scanner with deep-learning reconstruction and new bow-tie filter. British Journal of Radiology, 2022, 95, .	2.2	0